Published in final edited form as:
Neuron. 2014 April 2; 82(1): 109–124. doi:10.1016/j.neuron.2014.02.015.

Calcineurin Signaling Regulates Neural Induction Through Antagonizing the BMP Pathway

Ahryon Cho[1], **Yitai Tang**[#1], **Jonathan Davila**[#2], **Suhua Deng**[1], **Lei Chen**[1], **Erik Miller**[3], **Marius Wernig**[2], and **Isabella A Graef**[1,*]

[1]Department of Pathology, Stanford University School of Medicine, 300 Pasteur Drive, Stanford, California 94305, USA

[2]Institute for Stem Cell Biology and Regenerative Medicine, Stanford University School of Medicine, Stanford, California 94305, USA

[3]Department of Genetics, Stanford University School of Medicine, 300 Pasteur Drive, Stanford, California 94305, USA

[#] These authors contributed equally to this work.

Summary

Development of the nervous system begins with neural induction, which is controlled by complex signaling networks functioning in concert with one another. Fine-tuning of the bone morphogenetic protein (BMP) pathway is essential for neural induction in the developing embryo. However, the molecular mechanisms by which cells integrate the signaling pathways that contribute to neural induction have remained unclear. We find that neural induction is dependent on the Ca^{2+}-activated phosphatase calcineurin (CaN). FGF-regulated Ca^{2+} entry activates CaN, which directly and specifically dephosphorylates BMP-regulated Smad1/5 proteins. Genetic and biochemical analyses revealed that CaN adjusts the strength and transcriptional output of BMP signaling and that a reduction of CaN activity leads to an increase of Smad1/5-regulated transcription. As a result, FGF-activated CaN signaling opposes BMP signaling during gastrulation, thereby promoting neural induction and the development of anterior structures.

Introduction

Embryonic development requires the concerted actions of multiple signaling pathways to control complex gene regulatory networks, which govern cell-fate decisions. The earliest step in the development of the nervous system, which is called “neural induction,” is the acquisition of a neural cell fate by a subset of ectodermal cells during gastrulation. Previous studies have shown that neural induction is a dynamic process, which requires the integration of a number of signaling pathways, including inhibition of the BMP pathway

[*]Correspondence to: Isabella Graef, Correspondence and requests for materials should be addressed to IAG (igraef@stanford.edu)..

(so-called default model) as well as coordinated regulation of FGF, Ca^{2+} and Wnt signaling (Levine and Brivanlou, 2007; Stern, 2005; Webb et al., 2005). However, it remains unresolved how these signaling pathways are integrated to induce the earliest neuroectodermal precursors.

Downregulation of BMP signaling within the prospective neural plate is the key step in neural induction and conserved from invertebrates to vertebrates. BMP signaling functions in a dose-dependent manner and is therefore tightly regulated during development to adjust pathway activity according to spatial and temporal context. This is well illustrated by mutant mouse lines with either increased or decreased BMP activity. Increased activity results in truncation of anterior structures and defects of forebrain development, while reduced activity leads to expansion of anterior neuroectoderm (Bachiller et al., 2000; Davis et al., 2004).

As a member of the TGF-β superfamily, BMP transmits intracellular signals through Smad proteins: receptor-regulated Smads (R-Smads; Smad1/5/8 for BMP and Smad2/3 for TGFβ/Nodal/Activin), common Smad4, and inhibitory Smads (Smad6/7). R-Smads have two conserved domains, MH1 (N) and MH2 (C), which are connected by a linker region. Upon ligand binding the C-terminal SXS motif of R-Smads is phosphorylated by the BMP receptor I kinase. This phosphorylation event triggers a conformational change of R-Smads resulting in nuclear translocation and activation of BMP-responsive genes (Feng and Derynck, 2005). BMP signaling is inhibited by extracellular antagonists, by interaction of R-Smads with Smad6/7 and by phosphorylation of the linker region of R-Smads, which promotes cytoplasmic retention and proteasomal degradation, thereby decreasing the pool of R-Smads (Feng and Derynck, 2005; Kretzschmar et al., 1997; Sapkota et al., 2007). The FGF and Wnt pathways have been shown increase phosphorylation of the linker region of R-Smads, thus antagonizing BMP signaling during neural induction of amphibian and chick embryos (Fuentealba et al., 2007; Kuroda et al., 2005; Pera et al., 2003).

Another key signaling pathway implicated in the regulation of neural induction is Ca^{2+} signaling. It has been shown that an increase of intracellular Ca^{2+} ($[Ca^{2+}]_i$) in the dorsal ectoderm of amphibian gastrulae is critical for neural induction (Batut et al., 2005; Leclerc et al., 2011; Leclerc et al., 2000; Moreau et al., 1994). Influx of extracellular Ca^{2+} via L-type Ca^{2+} channels and TRP channels as well as inositol 1,4,5-trisphosphate (IP_3) regulated Ca^{2+} release from intracellular stores is thought to underlie the increase of $[Ca^{2+}]_i$ during neural induction in amphibian embryos (Ault et al., 1996; Lee et al., 2009).

Although the key step in the activation of BMP-regulated transcription is C-terminal phosphorylation of R-Smads by the BMP-receptor, the reversal of Smad phosphorylation as a regulatory mechanism and the identity of Smad-specific phosphatases remain elusive. While the existence of nuclear phosphatases has been proposed and a number of constitutively active candidate phosphatases have been suggested by *in vitro* studies, mouse molecular genetics have thus far not provided a link to BMP signaling or a strong argument for or against the relevance these phosphatases *in vivo* (Bruce and Sapkota, 2012).

CaN is a Ca^{2+}/calmodulin (CaM)-dependent serine/threonine phosphatase, composed of a regulatory (CnB) and a catalytic (CnA) subunit, which is activated by an increase of $[Ca^{2+}]_i$. Three genes encode the catalytic subunit, CnA (*CnA* α, β, γ), while two genes, one ubiquitously expressed somatic (*CnB1*) and the other testis specific (*CnB2*), encode the regulatory subunit, CnB. CnA consists of an N-terminal phosphatase domain, a CnB binding motif, a CaM binding motif, and a C-terminal auto-inhibitory domain. CnB, which has four EF-hand Ca^{2+} binding motifs, is tightly associated with CnA. Binding of Ca^{2+} and CaM to the CaN phosphatase complex results in displacement of the autoinhibitory element and subsequent activation of phosphatase activity. Genetic deletion of *CnB1* eliminates all of CaN phosphatase activity in somatic cells (Neilson et al., 2004). CaN can be activated by Ca^{2+} entry through CRAC channels, L-type Ca^{2+} channels, Gap junctions and Trp channels (Bush et al., 2006; Graef et al., 1999). The membrane signals that have been shown to activate CaN include many receptor and non-receptor tyrosine kinases, membrane depolarization, G-protein coupled receptors and non-canonical Wnt signals (Wu et al., 2007). CaN has been shown to regulate a broad spectrum of developmental processes by activation of NFAT-dependent transcription, but is also well suited to intercalate with other signaling pathways.

In the present study, we demonstrate that CaN is essential for neural induction in human and murine embryonic stem cells (ESCs). We describe a new and unexpected role for CaN in regulating the strength and the transcriptional output of BMP signaling and show that CaN directly dephosphorylates the BMP-regulated Smad1/5 transcription factors. Mice lacking CaN activity show increased BMP activity and severe defects in the development of anterior neural structures. Our findings demonstrate that FGF-activated Ca^{2+}/CaN signaling antagonizes the BMP pathway and possibly reconciles the respective roles of FGF, Ca^{2+} and BMP-signaling during neural induction.

Results

CaN activity is required for neural induction during embryogenesis

We found that mice carrying a null mutation of *CnB1 (Ppp3r1)*, which eliminates all CaN activity in somatic cells (Neilson et al., 2004), displayed morphological defects that affected anterior neural structures. Scanning electron microscopy images taken at midgestation (E9.5, 22-24 somites) showed a size reduction of the *CnB1* mutant brain, which affected the prosencephalon most severely. Additional defects of head structures including the branchial arches, eyes and fronto-nasal prominence as well as an overall reduction of body size could be seen in mutant embryos (Figure 1A). Pax6 staining of E9.0 (18-20 somites) embryos showed that the prosencephalon of *CnB1* mutant embryos was misshapen and reduced to a small vesicle of thin neuroepithelium (Figure 1B).

The widespread defects in anterior structures seen in the mutant embryos led us to speculate that the initial specification of rostral neuroectoderm might be affected. To determine whether the morphological defects observed in mutant embryos start at gastrulation, we examined the expression of germlayer markers in neural plate stage (E7.5) control and mutant embryos. Gastrulation in the mouse embryo begins around E6.0 and results in the generation of the three germ layers, ectoderm, mesoderm and definitive endoderm, from

which all fetal tissues will develop (Tam and Loebel, 2007). In *CnB1* mutant embryos the expression of anterior neuroectoderm markers (*FezF1, FezF2,* and *Six3)* was significantly reduced compared to stage matched wild-type littermate controls (Figure 1C). In contrast, expression levels of the mesodermal marker *Brachyury* (*T*) and ectodermal marker *Krt8* were increased in mutant embryos, while there was no significant difference in the expression of the endodermal marker *Gata6* (Figure 1D-F).

To determine the time during development when CaN signaling was essential we used pharmacological inhibition of CaN with the highly specific and rapidly acting inhibitor of CaN phosphatase activity, cyclosporin A (CsA). CsA and FK506 are highly lipophilic, microbial products, which pass through the cell membrane, placenta or blood brain barrier. They bind to intracelluar immunophilins, producing inhibitory complexes that block CaN phosphatase activity at nanomolar concentrations. The exquisite specificity of CsA and FK506 for CaN is based upon the large composite surface used to bind the CaN complex (Griffith et al., 1995). CsA has been a valuable tool to dissect developmental roles of CaN *in vitro* and *in vivo*. In previous studies we and others have found that *in vivo* treatment of mice with CsA or FK506 phenocopies the null mutation of *CnB1* in a number of systems including vascular, lymphocyte, heart valve, neural and coronary artery development (Chang et al., 2004; Graef et al., 2001; Graef et al., 2003; Quadrato et al., 2012; Zeini et al., 2009). Injection of CsA into pregnant mice at E6.25 and E6.75 reproduced the developmental defects seen in *CnB1* mutant embryos and CsA-treated embryos were indistinguishable in gene expression from *CnB1* mutant embryos (Figure 1 H-K). As observed in the *CnB1* mutant embryos the expression of neuroectodermal markers *Six3, FezF1* and *FezF2* was dramatically reduced while expression of the mesodermal marker, *Brachyury*, was increased when CaN activity was inhibited on day 6 of gestation. Pax6 staining of CsA treated embryos revealed similar defects in forebrain development as observed in *CnB1* mutant animals (Figure 1L). These findings pointed towards a role of CaN in embryonic patterning during gastrulation. To examine the CnBl expression pattern during early embryonic development we performed immunohistochemical analysis and qRT-PCR studies of early mouse embryos. The highest levels of CnBl protein expression were seen in the hypoblast of E6.5 embryos (Figure S1A). *CnB1* mRNA was expressed during gastrulation and in murine ESCs, while *CnB2* was undetectable in somatic tissues and ESCs (Figure S1B-C).

Calcineurin activity is required for neural differentiation of ES cells

The molecular analysis of signaling in the early mouse embryo is limited by size and relative inaccessibility of the mammalian gastrula. *In vitro* differentiation of embryonic stem cells (ESCs) to neural progenitor cells (NPCs) provided a means for biochemical analysis of the mechanism of action of CaN in early neural development. Embryoid body (EB) cultures of ESCs recapitulate the process of germ-layer formation and generate cell lineages in a defined temporal pattern. Because *Sox1* is one of the earliest neural markers expressed specifically in the neural plate, we used Sox1-GFP knock-in mESCs to monitor and quantify neural induction *in vitro* (Ying et al., 2003) (Figure 2A).

Using fluorescence activated cell sorting (FACS) we found that inhibition of CaN with a combination of FK506 and CsA (FK/CsA) during the differentiation period (d3-12) severely

compromised differentiation of ESCs into GFP-positive NPCs (Figure 2B-C). We used a combination of FK506 and CsA, because the level of CaN expression in mEBS is high (for a more detailed explanation see the Supplemental Information). The concentration of inhibitors used was based on their ability to completely inhibit CaN phosphatase activity, using the phosphorylation state of the well-established CaN substrate, NFATc4 as a read-out for CaN activity (Figure S2A). The failure of neural differentiation of FK/CsA treated mESCs was consistent with the defects in neural development observed in *CnB1* mutant and CsA-treated embryos and suggested that CaN activity is required for neural differentiation of mESCs.

To gain insight into the molecular mechanisms underlying CaN's role in neural induction we defined the critical time-window during ESC to neuron differentiation that was sensitive to inhibition of CaN activity (Figure 2D). Addition of FK/CsA for defined periods followed by compound wash-out revealed that FK/CsA treatment from d3-8 inhibited ESC differentiation into *Sox 1*-GFP-positive NPCs (Figure 2E). Subsequent culture for 7–16 days without FK/CsA did not reverse this block (Figure 2F and S2F). Exposure to FK/CsA after 8 days of differentiation failed to inhibit GFP-expression (Figure 2E). As further confirmation that the effect of FK/CsA on neural induction was the result of inhibiting CaN activity, we used a cell-permeable dimer of FK506, FK1012 (Spencer et al., 1993), which interacts with FKBP12 at a stoichiometry of 1:2 (Kd=0.5nM), but does not bind to or inhibit CaN. This compound had no effect on neural induction of mESCs (Figure 2E). Pharmacological inhibition of CaN had a dose dependent effect upon neural induction (Figure S2B-C), which further confirmed that that the effect on neural induction seen following treatment of EBs with FK/CsA, was indeed due to inhibition of CaN activity.

Co-staining mEB cultures on d12 for the early neuroectodermal markers Pax6 and Nestin corroborated the FACS and Western blot data. CaN inhibition from d3-8 resulted in the absence of NPCs double-positive for *Sox1*-GFP and Pax6 or Nestin (Figure S2E). After dissociation and further culture for 3 days, non-treated (NT) cells underwent efficient neurogenesis leading to the generation of βIII-tubulin-positive post-mitotic neurons. However, cultures that were exposed to FK/CsA from d3-8 showed no βIII-tubulin-positive cells on d15 (Figure 2F) or on d24 (Figure S2F), indicating that inhibition of CaN did not simply delay neural induction.

To investigate the role of CaN signaling in human neuroectoderm formation, H1-human ESCs (hESCs) were differentiated into NPCs. Early neural differentiation of hESC was characterized by the formation of neural rosette structures that expressed Sox2 and PLZF (Figure 2G, upper panel) on d11 of hEB differentiation. Treatment of hESC with FK/CsA blocked the induction of $Sox2^{+}/PLZF^{+}$ NPCs and resulted in the appearance flat cuboidal cells (Figure 2G, lower panel).

Microarray analysis of mEBs on d4, d6, d8 and d12 of differentiation revealed that CaN inhibition specifically reduced neural lineage markers, which were expressed at very low levels on d12 in FK/CsA-treated cells when compared to NT controls (Figure 2H and S2I-K). In contrast, the expression of pluripotency (*Nanog, Oct4 & Rex1*), mesoderm (*Brachyury, Gsc & GATA1*), endoderm (*Sox7, Sox17, HNF1α),* and ectoderm (*Krt8, Krt18,*

Tcfap2a) markers was not significantly changed by CaN inhibition during mEB differentiation (Figure 2I and S2L). NFATc4 phosphorylation and Sox1, GFP, Nova and BLBP were used to monitor CaN activity and neural differentiation in samples used for microarray analysis (Figure S2D and S2H-J). These results indicate that lack of CaN activity altered both murine and human cells in a manner that prevented later neuronal differentiation.

FGF8 regulated Ca^{2+} entry enhances neural induction

Because CaN is activated by signals, which increase the concentration of $[Ca^{2+}]_i$, we sought to define the source of the Ca^{2+}-signal that activated CaN during neural induction. A number of studies support a role for FGF signaling during acquisition of a neural cell fate *in vivo* and *in vitro* (De Robertis and Kuroda, 2004; Stern, 2005; Wilson et al., 2000), but the emerging picture of how FGFs promote neural induction seems to be complex. During embryogenesis, *Fgf8* and *Fgf17* are expressed in prestreak- and streak-stage embryos (Crossley and Martin, 1995) and FGF signaling in epiblast cells was found to repress *BMP4 and BMP7* mRNA expression (Wilson et al., 2000). FGFs have also been shown to attenuate BMP signaling intracellularly and to increase the size of the neural plate in amphibian embryos (Pera et al., 2003) as well as to act independently of BMPs (Delaune et al., 2005; Stern, 2005). In addition, it has been shown that treatment of hESCs with a FGFR tyrosine kinase inhibitor blocks neural induction in a dose-dependent manner, suggesting that FGF signaling is also critical for neural induction of hESC (LaVaute et al., 2009).

FACS analyses showed that treatment of mEBs with FGF8 and FGF17 during the FK/CsA sensitive time period, d3-8, significantly increased the number of *Sox1*-GFP-positive cells (Figure 3A) compared to NT samples. Western blot analysis of these cells confirmed increased expression of GFP and Sox1 (Figure 3B). In contrast, treatment with FGF2 and FGF4 had a small inhibitory effect (Figure 3C-D), consistent with recent observations made during neural differentiation of human ESCs (Greber et al., 2011). These findings align well with distinct functions of FGF8 and FGF2 during early neural development (De Robertis and Kuroda, 2004; Stern, 2005).

Treatment of EBs with FGF8/17 could not bypass the requirement for CaN signaling during the differentiation of both hESCs and mESCs and enhanced neural induction by FGF8 required CaN activity (Figure 3E-G). There are two possible explanations for this finding. CaN activity could be required for cells to be competent to respond to FGF8 signaling or CaN could be a critical signaling intermediate in the intracellular FGF8 signal transduction cascade. The mRNA expression levels of FGF-receptors as well as of a number of known FGF-regulated genes were not changed in the FK/CsA treated samples (Figure S3). In addition, we have previously found that FGF8 directly activates CaN signaling in embryonic cortical neurons (Arron et al., 2006). Therefore, we concluded that CaN might be a key mediator of FGF8 signaling during neural induction.

It has been demonstrated that FGF signaling can promote Ca^{2+} entry through transient receptor potential (Trp) channels and that CaN is activated by Trp-channel mediated rise of intracellular Ca^{2+} (Fiorio Pla et al., 2005; Poteser et al., 2011). Therefore we tested whether Trp-channels were critical for differentiation of ESCs to NPCs. Phospholipase-Cγ1

(PLCγ1) is known to be recruited via its SH2 domain to phospho-tyrosine in the cytoplasmic tail of FGFRs, resulting in PLCγ1 activation, stimulation of phosphatidylinositol (PI) hydrolysis and the generation of the two second messengers, diacylglycerol (DAG) and IP_3 (Mohammadi et al., 1991). The Trp cation channel family (Trpc) is subdived into 4 groups: Trpc1; Trpc2; Trpc4 and c5; and Trpc3, c6 and c7. The Trpc3, c6 and c7 subfamily is directly activated by DAG (Hofmann et al., 1999), thereby coupling receptor/PLCγ signaling to Ca^{2+} entry. We found that inhibition of Trpc3 with the small molecule Pyr3 (Kiyonaka et al., 2009) blocked neural induction as well as the increase in neural differentiation brought about by FGF8 treatment (Figure 3G). These findings suggested that Ca^{2+} entry via Trpc3 might be critical for the activation of CaN by FGF8 during neural induction.

Inhibition of CaN enhances BMP signaling during ES cell differentiation

Microarray analysis of genes, differentially expressed in FK/CsA-treated and NT mEBs during the time period sensitive to CaN inhibition (d3-8), revealed a significant enrichment of BMP-responsive genes, including *Msx1*which had previously been shown to inhibit neuralization (Suzuki et al., 1997)(Figure 4A, Table S1 and Figure S4A). Consistent with the increased mRNA levels of *Bmp4* (Figure 4A), which is known to be under positive feedback regulation of BMP signaling (Karaulanov et al., 2004; Ramel and Hill, 2012), we found that treatment of mEBs with FK/CsA from d3-d8 of differentiation increased the expression of genes within the co-regulated Bmp4 synexpression cluster such as *Smad6*, *Msx1*, and *Msx2* which are direct transcriptional targets of BMP4-Smad1/5 signaling (Figure 4A and Figure S4A). These results pointed towards increased activation of the BMP pathway following inhibition of CaN activity during ESC differentiation. This finding was intriguing, given the known link between BMP signaling and neural induction. Seminal experiments, which led to the so called “default model” of neural induction showed that inhibition of BMP signaling during gastrulation was necessary and sufficient for neural induction in frog embryos. Secreted factors such as noggin or chordin directly bind to and neutralize BMPs during gastrulation and induce neural tissue in xenopus embryos (Hemmati-Brivanlou and Melton, 1994; Lamb et al., 1993; Sasai et al., 1995). Knock-out studies in mice have shown that the extracellular BMP inhibitors *chordin* and *noggin* are functionally redundant during early embryogenesis and are required for anterior neural differentiation (Bachiller et al., 2000).

Strikingly the effects of FK/CsA and of BMP4 treatment from d3-d8 were equivalent and both prevented differentiation of mESCs into *Sox1*-GFP-positive NPGs (Figure 4B). The opposite effect was seen in cultures treated with the BMP inhibitor Noggin (Figure 4B). Similar to the time window that we identified as critical for CaN activity (Figure 2), the effectiveness of BMP treatment in altering cell fate during mESC differentiation has been reported to be limited to a period prior to the onset of neural differentiation (Finley et al., 1999). In the early mouse embryo Flk1(Kdr), which at later stages is a well-known marker for cardiovascular and hematopoietic progenitors, is highly expressed in multipotent mesodermal progenitors that exit from the posterior primitive streak (Ema et al., 2006). Inhibition of CaN activity or exposure to BMP4 led to a dramatic increase of cells expressing Flk1, while Noggin inhibited differentiation into Flk1-positive cells (Figure 4B

and Figure S4A). In addition, FK/CsA treatment increased the expression of posterior primitive streak markers (*Mesp1, HoxB1*), suggesting the enrichment of more posterior mesoderm populations, while anterior streak makers (*Cer1, Chrd*) were reduced (Figure S4A). Similar observations had been made during *in vitro* differentiation of ESCs in the presence of BMP4 (Nostro et al., 2008). The high expression of Flk1, along with the increased expression of *Tie2, PFGR*α and *Nrp1* at d12 might reflect enhanced differentiation of FK/CsA treated mESCs along the vascular lineage. Markers that delineate other cell types that arise from Flk1-positive mesodermal progenitors, including hematopoietic (*Tal1, Itga2b, Gata1, Runx1, Hbb-y*), myocardial (*Nkx2-5, Mef2C, Tnnt2*), paraaxial and somitic lineages (*Tbx18, Tbx6, Pax3*) were not changed in FK/CSA treated cultures at d12 (Figure S4A). These data suggest that inhibition of CaN increases the intensity of BMP signaling during mESC differentiation.

CaN antagonizes BMP signaling by direct dephosphorylation of Smad1/5 proteins

To further delineate the functional relationship between CaN and BMP signaling we tested whether inhibition of BMP signaling proximal to binding its receptor with the BMP antagonist, Noggin, could bypass the requirement for CaN phosphatase activity during neural differentiation of mESCs. We found that, even in the presence of exogenously added Noggin, FK/CsA treatment reduced differentiation of mESCs into *Sox1*-GFP-positive NPCs (Figure 4C). This result suggested that CaN might modulate the BMP signaling pathway after binding of BMP proteins to the BMP receptor complex.

Signal transduction pathways are often regulated by dynamic interplay between protein kinases and phosphatases. Thus we focused our attention on the phosphorylation state of Smad1/5 proteins. Phosphorylations of serine residues in the linker (S206) and C-terminal (S463/465) region of the BMP-regulated Smad1/5 proteins regulate their transcriptional activity and stability (Massague et al., 2005). The level of C-terminal phosphorylation (pSmad1/5$^{C\text{-}term}$), which regulates nuclear translocation and activation of Smad-regulated transcription, determines the intensity of BMP signaling (Feng and Derynck, 2005). Treatment of mEBs with FK/CsA resulted in a pronounced increase of pSmad1/5$^{C\text{-}term}$ (Figure 4D, lane 2). As expected, treatment with Noggin reduced pSmad1/5$^{C\text{-}term}$ to an undetectable level (Figure 4D, lane 3). The level of phosphorylation following treatment with Noggin in the presence of FK/CsA was lower than in NT samples but higher than in samples treated with Noggin alone (Figure 4D, lane 4). The differences in pSmad1/5$^{C\text{-}term}$ levels might account for the dramatic differences in the number of *Sox1*-GFP-positive cells seen on d12 (Figure 4C). These epistasis experiments suggested that C-terminal phosphorylation sites in Smad1/5 might be critical targets of CaN signaling during ESC to NPC differentiation.

To examine the subcellular localization of pSmad1/5$^{C\text{-}term}$ after inhibition of CaN EBs were treated with for 1 hour with the FK/CsA, separated into nuclear and cytosolic fractions and analyzed for levels of total Smad1/5 and pSmad1/5$^{C\text{-}term}$ (Figure 4E). Endogenous CaN in mEBs was present in both the nuclear and cytoplasmic fractions (Figure 4E). We found that short treatment with FK/CsA or BMP4 resulted in increased pSmad1/5$^{C\text{-}term}$, which was most pronounced in the nuclear fraction. Treatment with okadaic acid (OA), which inhibits

the phosphatases PP1 and PP2A, had no effect on pSmad1/5$^{C\text{-}term}$, which indicated that the effect of CaN on pSmad1/5$^{C\text{-}term}$ was direct and not mediated by modulation of PP1 or PP2A activity (Figure 4E). Inhibition of CaN had only a minor effect on linker phosphorylation (Figure 4E). Total Smad1/5 protein levels did not change during this period. Interestingly, inhibition of CaN had no effect on the level of C-terminal phosphorylation of the Nodal/TGF-β/Activin-regulated R-Smads, Smad2/3 (Figure S5). These data suggest that the effects of CaN were exclusive to BMP-regulated R-Smads. To investigate whether regulation of Smad1/5 by CaN is unique to EBs, we examined HaCaT cells. Consistent with regulation of the intensity of the BMP signal by CaN, short-term treatment of HaCaT cells with FK/CsA increased basal pSmad1/5$^{C\text{-}term}$ as well as pSmad1/5$^{C\text{-}term}$ following stimulation with low levels of BMP2 (Figure 4F and S4B) and slowed the decay of the pSmad1/5$^{C\text{-}term}$ signal following the washout of BMP2 (Figure S4C).

Increased *Bmp4* mRNA expression, which we observed following prolonged inhibition of CaN activtiy (Figure 4A), could have auto/paracrine effects on the level of pSmad1/5$^{C\text{-}term}$. Thus, we examined whether short-term FK/CsA treatment, which resulted in a profound increase of pSmad1/5$^{C\text{-}term}$, had an effect on BMP4 transcription (Figure 4D-F, Figure S4B-C). We found no increase of *Bmp4* mRNA levels after short-term (1hr) inhibition of CaN activity (Figure S4D) suggesting that the role of CaN in the regulation of Smad1/5$^{C\text{-}term}$ phosphorylation is direct.

As an alternative approach to address the question whether CaN directly regulates Smad1/5$^{C\text{-}term}$ phosphorylation, we examined pSmad1/5$^{C\text{-}term}$ levels in hESCs expressing a constitutively active form of CaN. Active CaN is a truncated form of the catalytic Aα subunit, which lacks the autoinhibitory and a portion of the CaM-binding domain, but retains the CnB-binding domain(O'Keefe et al., 1992). This deletion renders CaN activity independent of Ca^{2+}. We infected hESCs with lentiviral vectors containing either GFP only (control) or active CaN and found that the normalized level (normalized on the expression of Smad1/5) of pSmad1/5$^{C\text{-}term}$ was ~4 fold lower in cells expressing active CaN compared to control cells (Figure 4G, top left panel). The phosphorylation state of the well-characterized CaN substrate NFATc4 was used as a positive control (Figure 4G, top right panel).

We next determined whether Smad1/5 proteins were direct substrates for CaN and tested whether CaN dephosphorylated Smad1/5 *in vitro* (Figure 4H). To obtain Smad1/5 proteins that were phosphorylated under physiological conditions we prepared extracts from d8 mEBs that were stimulated for 1 hour with 50 ng/ml BMP4. These extracts, which contained abundant amounts of pSmad1/5$^{C\text{-}term}$, were used as the substrate for *in vitro* phosphatase assays with recombinant CaN and CaM. Incubation of both nuclear and cytoplasmic extracts resulted in efficient C-terminal dephosphorylation of Smad1/5 by CaN (Figure 4H, top panel). Calf intestinal phosphatase, which is a robust, nonspecific phosphatase that dephosphorylates nucleotides, proteins, and alkaloids, was used as a positive control. The level of total Smad1/5 protein was not changed by incubation with CaN indicating that the loss of the pSmad1/5$^{C\text{-}term}$ signal seen in the immunoblot (Figure 4H, top panel) was due to direct dephosphorylation and not degradation of Smad1/5 (Figure 4H, second panel). Taken together, these results provide strong evidence that Smad1/5 proteins are direct targets of

CaN phosphatase activity and indicate that during the ES cell to NPC differentiation period, CaN dampens BMP signaling by dephosphorylating pSmad1/5$^{C\text{-}term}$, thus promoting induction of a neural cell fate.

Smad1/5 proteins are the critical targets of CaN during neural induction

One of the best-characterized developmental targets of CaN is the NFATc family of transcription factors. To test whether the BMP-regulated Smad1/5 proteins are indeed the critical targets of CaN phosphatase activity during neural induction, we generated mice that carry mutant alleles of all four NFATc genes, *NFATc1*$^{L/L}$ *c2*$^{-/-}$ *c3*$^{L/L}$*c4*$^{-/-}$, which we will refer to as QKO^{cond}. In order to investigate the role of NFAT-dependent transcription and to completely remove all four NFATc proteins during neural induction, we prepared an ESC line from the QKO^{cond} mice. We transfected this line with a 4-hydroxytamoxifen (4-OHT)-regulated form of Cre recombinase, which enabled us to acutely delete *NFATc1* and *NFATc3* by homologous recombination following 4-OHT treatment. We confirmed the lack of NFATc2 and NFATc4 expression and the 4-OHT-dependent deletion of *NFATc1* and *NFATc3* in the QKO^{cond} ESC line by qRT-PCR and Western blotting (Figure 5A and S6). Inhibition of CaN activity with FK/CsA in EBs, which lacked all four NFATc proteins, resulted inã 3-5 fold increase of pSmad1/5$^{C\text{-}term}$ (normalized to Smad1/5 expression levels) (Figure 5A, lane 4). These results indicate that the effect of CaN on C-terminal phosphorylation of Smad1/5 was independent of the expression of NFATc proteins. Immunoblot analysis of Sox1 expression on d12 of neural induction showed that neural induction was not impaired in 4-OHT treated QKO^{cond} EBs (Figure 5B). Treatment of QKO^{cond} EBs with FK/CsA blocked neural induction, as evidenced by the lack of Sox1 expression (Figure 5B), which is consistent with the hypothesis that Smad1/5 rather than NFATc proteins are the critical targets of CaN phosphatase activity during neural induction.

To further investigate the relationship between CaN and BMP signaling during neural induction, we asked whether CaN activity was required in the absence of BMP signaling. This was addressed by making use of small molecule inhibitors of the BMP type I receptors ALK2, ALK3 and ALK6, which block BMP-mediated phosphorylation of Smad1/5/8 (Yu et al., 2008). FACS analysis of *Sox1*-driven GFP expression following neural differentiation of 46C cells showed that both Dorsomorphin and LDN193189 strongly enhanced neural induction of mESCs (Figure 5C). Neither inhibition of CaN signaling nor addition of FGFs from d3 to d8 had any effect on neural induction when BMP receptor I kinase activity was fully inhibited with either Dorsomorphin or LDN193189 (Figure 5C).

While NT hESCs showed increased expression of SOX2 and PLZF following neural differentiation (Figure 5D, first panel), induction of neuronal markers was not detected in cultures that were differentiated in the presence of FK/CsA (Figure 5D, second panel). As observed during neural differentiation of mESCs (Figure 5C), differentiation of hESCs via the dual SMAD-inhibition protocol using LDN-193189 and SB431542, which robustly induced SOX2^{+}/PLZF^{+} NPCs precursors (Figure 5D, third panel) also bypassed the need for CaN signaling during neural induction (Figure 5D, fourth panel).

Given the requirement of Ca^{2+} for the activation of CaN and the block in neural induction that we observed following Pyr3 treatment of mEBs from d3-8, we tested whether

intracellular Ca^{2+} levels affected the phosphorylation state of Smad1/5. Treatment of EBs with the a Ca^{2+} ionophore dramatically decreased the level of pSmad1/$5^{C\text{-}term}$, an effect that was blocked by CaN inhibition (Figure 5E). Similarly, addition of FGF8 to mEBs also reduced pSmad1/$5^{C\text{-}term}$ levels. Since several FGF family members were expressed at high levels in mEBs during critical time-window of ESC to neuron differentiation (Figure S3), we tested whether inhibition of auto/paracrine FGF signaling with FGFR-Fc fusion proteins affected the levels of pSmad1/$5^{C\text{-}term}$. Interestingly, we found that treatment with FGFR-Fc fusion proteins or Trpc3 inhibition with Pyr3, increased the levels of pSmad1/$5^{C\text{-}term}$ (Figure 5E). These results suggested that the levels of pSmad1/$5^{C\text{-}term}$ were modulated by FGF/Trpc/Ca^{2+} dependent activation of CaN.

CaN opposes BMP-signaling during early embryonic development

To test whether a loss of CaN activity is correlated with increased BMP signaling during embryogenesis, we measured the expression levels of known BMP target genes in *CnB1* mutant and CsA treated embryos. Consistent with the results found during ESC to NPC differentiation, expression of the BMP-regulated genes, *Smad6* and *Mixl1*, was significantly increased in *CnB1* mutant E7.5 embryos (Figure 6A). Likewise, *Smad6* and *Mixl1* in E7.5 embryos that had been treated with CsA *in utero* on day 6 of gestation showed significantly increased expression of *Smad6* and *Mixl1* mRNAs (Figure 6B). *In vivo* and *ex vivo* studies have illustrated the essential role of BMP signaling in early cardiogenesis. Conditional deletion of *BmpR1a* in cardiac progenitors prevented formation of the cardiac crescent at E7.5 (4 somites) (Klaus et al., 2007) and application of BMP2 or BMP4 promoted (Schultheiss et al., 1997), while application of Noggin inhibited (Schlange et al., 2000) cardiac differentiation in chick embryos. Thus we examined the mRNA levels of genes expressed in early cardiac precursors. We found that expression of the earliest cardiac mesoderm marker, *Eomes* (Costello et al., 2011), was significantly increased in *CnB1* mutant and CsA treated E7.5 embryos (Figure 6A and B). Eomes directly activates *Mesp1* expression, which is one of the earliest molecular markers for cardiac progenitors and a master regulator of cardiovascular differentiation (Bondue et al., 2008). Consistent with the increased level of *Eomes* the mRNA level of *Mesp1* was also significantly upregulated in *CnB1* mutant and CsA treated embryos (Figure 6A and B).

To establish whether Smad1/$5^{C\text{-}term}$ was dephosphorylated by endogenous CaN during gastrulation we treated pregnant females on E7.0 embryos with CsA and harvested the embryos 2 hours after injection. Examination of Smad1/5 C-terminal phosphorylation showed a significant increase in pSmad1/$5^{C\text{-}term}$ levels in the treated embryos (Figure 6C). These results indicate that CaN actively opposes BMP signaling during gastrulation. To further evaluate the role of endogenous CaN in BMP signaling during early embryogenesis we examined Smad1/5 in *CnB1* mutant embryos and found increased levels of pSmad1/$5^{C\text{-}term}$ in *CnB1* mutant E8.0 headfolds (Figure 6D). In addition the level of Sox1 protein expression was reduced in *CnB1* mutants, which might reflect decreased neural induction due to increased activation of BMP signaling in the absence of CaN.

DISCUSSION

We have presented genetic and pharmacologic evidence that signaling through CaN is critical for neural induction during embryonic development and ES cell differentiation. Our *in vitro* studies show that the Ca^{2+}/CaN pathway regulates the strength of BMP signaling by direct and specific dephosphorylation of Smad1/5. We further find that inhibition of CaN signaling results in a cell fate change and directs mESCs towards the cardiovascular rather than neural lineage. Lastly we demonstrate that endogenously activated CaN dephosphorylates Smad1/5 during gastrulation. These findings support a model of neural induction in which activation of CaN by FGF-regulated Ca^{2+} entry via Trp channels opposes BMP signaling (Figure 7). In this model, Ca^{2+}/CaN functions downstream of R-Smad phosphorylation and dephosphorylation of R-Smads by CaN results in reduction of Smad-regulated transcription. Placing CaN function downstream of Smad complex formation allows for precise control of active Smad complexes, which positions CaN to be a point of convergence for integrating BMP signaling with other pathways that increase $[Ca^{2+}]_i$.

Calcineurin Signaling is Required for Neural Induction

Studies of neural induction in several model organisms have lead to both the default model as well as to more complex instructive models. In the default model cells adopt a neural cell fate in the absence of extrinsic signals. Elegant experiments in frogs showed that repression of BMP signaling by extracellular antagonists is required for neural differentiation in the embryo (Hemmati-Brivanlou and Melton, 1994; Lamb et al., 1993; Sasai et al., 1995). However, a number of findings have suggested that the default model might be too simple and that other signaling pathways, most notably FGF and Ca^{2+} signaling, have a modulating and/or instructive role during neural induction (Lamb and Harland, 1995; Sheng et al., 2003; Stern, 2005; Webb et al., 2005), which prompted us to study the mechanistic basis of signal integration during neural induction.

Most of the research on the role of Ca^{2+} signaling in neural induction has been done in amphibians. It was shown that during gastrulation $[Ca^{2+}]_i$ levels rise in dorsal but not ventral ectoderm and that Ca^{2+} entry via L-type Ca^{2+} channels and Trp channels might be critical for neural induction (Leclerc et al., 2011). Other studies described that at the onset of gastrulation there is an increase in IP_3 levels in the presumptive neuroectoderm pointing towards activation of IP_3/Ca^{2+} signaling (Kume et al., 1997). It has also been shown that inhibition of IP_3R signaling results in stage-specific changes in body axis patterning. When signaling was blocked at the gastrula stage frog embryos showed increased ventralization and a reduction of anterior structures (Yamaguchi and Shinagawa, 1989). The observed reduction of anterior structures is reminiscent of the findings in the CnB1 mutant mice. In addition, activation of CaN/NFATc signaling by IP_3/Ca^{2+} has been shown to be a negative regulator of canonical Wnt signaling thereby promoting ventral cell fates (Saneyoshi et al., 2002). However, our studies in mouse embryos, mESCs and hESCs show that during mammalian neural induction CaN integrates FGF-Ca^{2+} signaling at the level of C-terminal phosphorylation of Smad1/5 rather than working through the NFATc family of transcription factors.

Mice mutant for *CnB1* and mice in which CaN function was blocked during gastrulation by pharmacological inhibition with CsA, display defects in anterior neuroectoderm induction (Figure 1). In addition, inhibition of CaN activity during the differentiation of ESCs completely blocks neural induction (Figure 2). The *in vivo* as well as the *in vitro* inhibition of CaN with CsA indicate that CaN activity is required during a defined time window of development, which precedes the initial specification of neuroectoderm. The observed defects could reflect either an intrinsic requirement for CaN activity in neuroectodermal progenitors or a failure of surrounding cells to secrete a factor required for neural differentiation. Our finding that CaN directly modulates the strength of BMP signaling favors a cell autonomous role of CaN during neural induction.

This is further supported by the observation that CaN activity is required for FGF8 to enhance neural induction of ESCs (Figure 3). Interestingly anterior defects, including reduction of the prosencephalon, eyes, olfactory placodes and frontonasal structures, which resemble the phenotype of *CnB1* mutant embryos, have also been associated with a reduction of FGF8 expression (Meyers et al., 1998). However, these findings do not exclude the possibility of additional roles for CaN in surrounding tissues, such as the nascent mesoderm and definitive endoderm.

Calcineurin Modulates the Strength of BMP Signaling

Precise regulation of the intensity and duration of BMP signaling, which is subject to modulation by other signaling pathway, is critical for specific gene expression patterns underlying developmental decisions. The results presented in this manuscript shed new light on how Ca^{2+} signaling intersects with the BMP pathway. Our *in vitro* and *in vivo* studies indicate that in the absence of CaN activity the expression of BMP-regulated genes is increased, which suggests that CaN modulates either the intensity or the duration of BMP signaling. Both the intensity and duration of BMP signaling can be controlled through phosphorylation of Smad proteins. Phosphorylation of the linker region by MAPK and GSK3 enhances degradation of Smad1 and reduces the duration of BMP signaling (Kretzschmar et al., 1997; Kuroda et al., 2005; Sapkota et al., 2007). Phosphorylation of the C-terminus of R-Smads by the type I receptor determines the intensity of BMP signaling, but little is known about how other signaling pathways might intersect with the BMP pathway to regulate its signal intensity. We found that CaN reduces the intensity of BMP signaling by direct dephosphorylation of R-Smad$^{C\text{-term}}$. Our genetic and pharmacologic data show that CaN dephosphorylates Smad1/5$^{C\text{-term}}$ during early embryonic development of mice and during neural differentiation of ESCs.

Interestingly, we found little evidence that the linker region of Smad1 is a substrate for CaN during neural induction. Notably, EBs also showed no detectable increase of pSmad2/3$^{C\text{-term}}$ following inhibition of CaN (Figure S5 and supplemental text). These studies indicate that CaN is specific for the BMP branch of the TGFβ superfamily. Remarkably, up to date, no R-Smad phosphatases, which are regulated by signaling pathways that oppose the BMP pathway, have been identified and confirmed by genetic studies. Our finding that BMP signaling is inhibited by CaN indicates that the default and instructive models are not mutually exclusive. Rather the instructive signals that increase intracellular Ca^{2+} levels and

activate CaN (and other pathways) also reduce constitutive BMP signaling by dephosphorylation of Smad1/5$^{C\text{-}term}$. Thus it appears that the integrative functions of CaN provide an essential step in neural induction by bringing the default pathway under local inductive influences provided by FGF signaling.

For a number of reasons we hypothesize that the role of CaN in neural induction is cell autonomous. First, short-term inhibition of CaN activity in ESCs, HaCaT cells and early mouse embryos resulted in pronounced hyperphosphorylation of pSmad1/5$^{C\text{-}term}$ (Figure 4-6 and S4). Second, we found that pSmad1/5$^{C\text{-}term}$ proteins were direct substrates of CaN phosphatase activity (Figure 4H). Third, overexpression of active CaN in human EBs significantly lowered the level of pSmad1/5$^{C\text{-}term}$ (Figure 4G). Lastly, while we saw increased levels of BMP4 expression after long-term inhibition of CaN, the levels of BMP4 mRNA were not elevated following short-term inhibition with FK/CsA (Figure S4D). The increase of BMP4 mRNA expression following prolonged inhibition of CaN activity is not unexpected, as it is well known that Bmp4 transcription is under positive feedback regulation (Karaulanov et al., 2004; Ramel and Hill, 2012). However, all the experiments on Smad1/5$^{C\text{-}term}$ phosphorylation were performed after short-term treatments with FK/CsA, at timepoints during which the levels of Bmp4 mRNA were not increased.

Calcineurin Antagonizes BMP Signaling during Gastrulation

Lineage specification during embryonic development is controlled by the coordinated activation and inhibition of signaling pathways. Several lines of evidence strongly argue that CaN directly opposes BMP signaling during gastrulation. First, embryonic patterning defects of mice lacking CaN activity were reminiscent of mice carrying mutations in BMP antagonists and of mice with increased BMP activity (Bachiller et al., 2000; Davis et al., 2004) (Figure 1). Second, the expression of BMP regulated genes was changed in *CnB1* mutant and CsA treated embryos (Figure 6). Third, BMP signaling is essential for the choice between ectodermal and mesodermal fates in mouse embryos and embryos mutant for *BMP4* and *BMPr1a* display ectopic neural differentiation accompanied by suppression of mesodermal cell fates (Di-Gregorio et al., 2007; Winnier et al., 1995). Consistent with an antagonistic effect of CaN on BMP signaling, *CnB1* mutant and CsA treated embryos showed significantly increased mesodermal and decreased neuroectodermal marker expression (Figure 1 and 6). Smad-regulated transcription is also implicated in differentiation of cardiac tissue from mesodermal precursors. The increased expression of *Eomes* and *Mesp1* suggests increased differentiation along the cardiogenic lineage in *CnB1* mutant and CsA treated embryos. Lastly, Smad1/5$^{C\text{-}term}$ was hyperphosphorylated in mouse embryos lacking CaN activity (Figure 6). In summary, our data indicate that CaN signaling is required during early embryonic patterning to antagonize BMP signaling thus promoting neuroectodermal and restricting mesodermal/cardiac differentiation.

A more speculative implication of our studies relates to how gradients of signaling are converted to discreet outcomes or to different cell fates. In the developing embryo BMP is produced locally and then converted to gradients. Cells within the gradient then develop discreet digital responses to the analogue gradient. These observations indicate that mechanisms exist that allow threshold discrimination and models involving feedback and

feed-forward controls have been developed and partially quantified. Our studies identify a new mechanism for setting a variable threshold for BMP signaling that would be dependent upon local FGF levels. Although we have called attention to FGF in inducing CaN activity, other sources of Ca^{2+}/CaN activation might also contribute to opposing BMP signaling in the early embryo, including GAP junctions and other Ca^{2+} channels. One prediction of our model is that loss of CaN activity might result in loss or change of cell fates in the developing embryo. Indeed this prediction does appear be satisfied in that the loss of neural fate seen in *CnB1*-deficient embryos is accompanied by increased conversion to certain mesodermal cell fates.

Experimental Procedures

Mouse lines and *in utero* CsA treatment

CnB1 mutant mice (Neilson et al., 2004) and *in utero* CsA treatment (Graef et al., 2001) were previously described.

In vitro differentiation of murine ESCs and human ESCs (hESCs)

Murine ESCs: 46C ESCs(Ying et al., 2003) were plated on gelatin-coated dishes in ESC medium supplemented with LIF. On d3, dissociated single cells were seeded into ultra-low attachment dishes in ESC medium and embryoid bodies (EBs) were plated on tissue culture dishes on d7. After 24 hours, the ESC medium was changed to ITS medium. Human ESCs: EBs were formed from a single cell suspension of H1 hESC in AggreWell™ plates (STEMCELL Technologies). The EBs were cultured in ultra-low attachment dishes for 4 days and plated on matrigel-coated dishes for 6 days. Cell culture conditions and small molecule treatments are detailed in Extended Experimental Procedures.

Flow Cytometry, microarray and data processing

FACS analysis using BD FACS Scan system and gene expression analysis using the Affymetrix Mouse Gene 1.0 ST arrays are detailed in Extended Experimental Procedures.

Quantitative real-time PCR, immublots, immunostaining, and *in vitro* phosphatase Assay

qRT-PCR was conducted using Power SYBR green PCR Master Mix (Applied Biosystems) and gene-specific primers listed in Table S2. Antibodies used for Western blots and immunostaining and i*n vitro* phosphatase assays are detailed in Extended Experimental Procedures.

Supplementary Material

Refer to Web version on PubMed Central for supplementary material.

Acknowledgments

We thank M.Fuller and G.Fishell for critically reading this manuscript. The 46C Sox1-GFP ESCs were a kind gift from Austin Smith, Cambridge. These studies were supported by a grant from the NIH to IAG (5PN2EY016525)

References

Arron JR, Winslow MM, Polleri A, Chang CP, Wu H, Gao X, Neilson JR, Chen L, Heit JJ, Kim SK, et al. NFAT dysregulation by increased dosage of DSCR1 and DYRK1A on chromosome 21. Nature. 2006; 441:595–600. [PubMed: 16554754]

Ault KT, Durmowicz G, Galione A, Harger PL, Busa WB. Modulation of Xenopus embryo mesoderm-specific gene expression and dorsoanterior patterning by receptors that activate the phosphatidylinositol cycle signal transduction pathway. Development. 1996; 122:2033–2041. [PubMed: 8681784]

Bachiller D, Klingensmith J, Kemp C, Belo JA, Anderson RM, May SR, McMahon JA, McMahon AP, Harland RM, Rossant J, et al. The organizer factors Chordin and Noggin are required for mouse forebrain development. Nature. 2000; 403:658–661. [PubMed: 10688202]

Batut J, Vandel L, Leclerc C, Daguzan C, Moreau M, Neant I. The Ca2+-induced methyltransferase xPRMT1b controls neural fate in amphibian embryo. Proc Natl Acad Sci U S A. 2005; 102:15128–15133. [PubMed: 16214893]

Bondue A, Lapouge G, Paulissen C, Semeraro C, Iacovino M, Kyba M, Blanpain C. Mesp1 acts as a master regulator of multipotent cardiovascular progenitor specification. Cell Stem Cell. 2008; 3:69–84. [PubMed: 18593560]

Bruce DL, Sapkota GP. Phosphatases in SMAD regulation. FEBS Lett. 2012; 586:1897–1905. [PubMed: 22576046]

Bush EW, Hood DB, Papst PJ, Chapo JA, Minobe W, Bristow MR, Olson EN, McKinsey TA. Canonical transient receptor potential channels promote cardiomyocyte hypertrophy through activation of calcineurin signaling. J Biol Chem. 2006; 281:33487–33496. [PubMed: 16950785]

Chang CP, Neilson JR, Bayle JH, Gestwicki JE, Kuo A, Stankunas K, Graef IA, Crabtree GR. A field of myocardial-endocardial NFAT signaling underlies heart valve morphogenesis. Cell. 2004; 118:649–663. [PubMed: 15339668]

Costello I, Pimeisl IM, Drager S, Bikoff EK, Robertson EJ, Arnold SJ. The T-box transcription factor Eomesodermin acts upstream of Mesp1 to specify cardiac mesoderm during mouse gastrulation. Nat Cell Biol. 2011; 13:1084–1091. [PubMed: 21822279]

Crossley PH, Martin GR. The mouse Fgf8 gene encodes a family of polypeptides and is expressed in regions that direct outgrowth and patterning in the developing embryo. Development. 1995; 121:439–451. [PubMed: 7768185]

Davis S, Miura S, Hill C, Mishina Y, Klingensmith J. BMP receptor IA is required in the mammalian embryo for endodermal morphogenesis and ectodermal patterning. Dev Biol. 2004; 270:47–63. [PubMed: 15136140]

De Robertis EM, Kuroda H. Dorsal-ventral patterning and neural induction in Xenopus embryos. Annu Rev Cell Dev Biol. 2004; 20:285–308. [PubMed: 15473842]

Delaune E, Lemaire P, Kodjabachian L. Neural induction in Xenopus requires early FGF signalling in addition to BMP inhibition. Development. 2005; 132:299–310. [PubMed: 15590738]

Di-Gregorio A, Sancho M, Stuckey DW, Crompton LA, Godwin J, Mishina Y, Rodriguez TA. BMP signalling inhibits premature neural differentiation in the mouse embryo. Development. 2007; 134:3359–3369. [PubMed: 17699604]

Ema M, Takahashi S, Rossant J. Deletion of the selection cassette, but not cis-acting elements, in targeted Flk1-lacZ allele reveals Flk1 expression in multipotent mesodermal progenitors. Blood. 2006; 107:111–117. [PubMed: 16166582]

Feng XH, Derynck R. Specificity and versatility in tgf-beta signaling through Smads. Annu Rev Cell Dev Biol. 2005; 21:659–693. [PubMed: 16212511]

Finley MF, Devata S, Huettner JE. BMP-4 inhibits neural differentiation of murine embryonic stem cells. J Neurobiol. 1999; 40:271–287. [PubMed: 10440729]

Fiorio Pla A, Maric D, Brazer SC, Giacobini P, Liu X, Chang YH, Ambudkar IS, Barker JL. Canonical transient receptor potential 1 plays a role in basic fibroblast growth factor (bFGF)/FGF receptor-1-induced Ca2+ entry and embryonic rat neural stem cell proliferation. J Neurosci. 2005; 25:2687–2701. [PubMed: 15758179]

Fuentealba LC, Eivers E, Ikeda A, Hurtado C, Kuroda H, Pera EM, De Robertis EM. Integrating patterning signals: Wnt/GSK3 regulates the duration of the BMP/Smad1 signal. Cell. 2007; 131:980–993. [PubMed: 18045539]

Graef IA, Chen F, Chen L, Kuo A, Crabtree GR. Signals transduced by Ca(2+)/calcineurin and NFATc3/c4 pattern the developing vasculature. Cell. 2001; 105:863–875. [PubMed: 11439183]

Graef IA, Mermelstein PG, Stankunas K, Neilson JR, Deisseroth K, Tsien RW, Crabtree GR. L-type calcium channels and GSK-3 regulate the activity of NF-ATc4 in hippocampal neurons. Nature. 1999; 401:703–708. [PubMed: 10537109]

Graef IA, Wang F, Charron F, Chen L, Neilson J, Tessier-Lavigne M, Crabtree GR. Neurotrophins and Netrins Require Calcineurin/NFAT Signaling to Stimulate Outgrowth of Embryonic Axons. Cell. 2003; 113:657–670. [PubMed: 12787506]

Greber B, Coulon P, Zhang M, Moritz S, Frank S, Muller-Molina AJ, Arauzo-Bravo MJ, Han DW, Pape HC, Scholer HR. FGF signalling inhibits neural induction in human embryonic stem cells. EMBO J. 2011; 30:4874–4884. [PubMed: 22085933]

Griffith JP, Kim JL, Kim EE, Sintchak MD, Thomson JA, Fitzgibbon MJ, Fleming MA, Caron PR, Hsiao K, Navia MA. X-ray structure of calcineurin inhibited by the immunophilin-immunosuppressant FKBP12-FK506 complex. Cell. 1995; 82:507–522. [PubMed: 7543369]

Hemmati-Brivanlou A, Melton DA. Inhibition of activin receptor signaling promotes neuralization in Xenopus. Cell. 1994; 77:273–281. [PubMed: 8168134]

Hofmann T, Obukhov AG, Schaefer M, Harteneck C, Gudermann T, Schultz G. Direct activation of human TRPC6 and TRPC3 channels by diacylglycerol. Nature. 1999; 397:259–263. [PubMed: 9930701]

Karaulanov E, Knochel W, Niehrs C. Transcriptional regulation of BMP4 synexpression in transgenic Xenopus. The EMBO journal. 2004; 23:844–856. [PubMed: 14963489]

Kiyonaka S, Kato K, Nishida M, Mio K, Numaga T, Sawaguchi Y, Yoshida T, Wakamori M, Mori E, Numata T, et al. Selective and direct inhibition of TRPC3 channels underlies biological activities of a pyrazole compound. Proc Natl Acad Sci U S A. 2009; 106:5400–5405. [PubMed: 19289841]

Klaus A, Saga Y, Taketo MM, Tzahor E, Birchmeier W. Distinct roles of Wnt/beta-catenin and Bmp signaling during early cardiogenesis. Proc Natl Acad Sci U S A. 2007; 104:18531–18536. [PubMed: 18000065]

Kretzschmar M, Doody J, Massague J. Opposing BMP and EGF signalling pathways converge on the TGF-beta family mediator Smad1. Nature. 1997; 389:618–622. [PubMed: 9335504]

Kume S, Muto A, Okano H, Mikoshiba K. Developmental expression of the inositol 1,4,5-trisphosphate receptor and localization of inositol 1,4,5-trisphosphate during early embryogenesis in Xenopus laevis. Mech Dev. 1997; 66:157–168. [PubMed: 9376319]

Kuroda H, Fuentealba L, Ikeda A, Reversade B, De Robertis EM. Default neural induction: neuralization of dissociated Xenopus cells is mediated by Ras/MAPK activation. Genes Dev. 2005; 19:1022–1027. [PubMed: 15879552]

Lamb TM, Harland RM. Fibroblast growth factor is a direct neural inducer, which combined with noggin generates anterior-posterior neural pattern. Development. 1995; 121:3627–3636. [PubMed: 8582276]

Lamb TM, Knecht AK, Smith WC, Stachel SE, Economides AN, Stahl N, Yancopolous GD, Harland RM. Neural induction by the secreted polypeptide noggin. Science. 1993; 262:713–718. [PubMed: 8235591]

LaVaute TM, Yoo YD, Pankratz MT, Weick JP, Gerstner JR, Zhang SC. Regulation of neural specification from human embryonic stem cells by BMP and FGF. Stem Cells. 2009; 27:1741–1749. [PubMed: 19544434]

Leclerc C, Neant I, Moreau M. Early neural development in vertebrates is also a matter of calcium. Biochimie. 2011; 93:2102–2111. [PubMed: 21742011]

Leclerc C, Webb SE, Daguzan C, Moreau M, Miller AL. Imaging patterns of calcium transients during neural induction in Xenopus laevis embryos. J Cell Sci. 2000; 113(Pt 19):3519–3529. [PubMed: 10984442]

Lee KW, Moreau M, Neant I, Bibonne A, Leclerc C. FGF-activated calcium channels control neural gene expression in Xenopus. Biochim Biophys Acta. 2009; 1793:1033–1040. [PubMed: 19135096]

Levine AJ, Brivanlou AH. Proposal of a model of mammalian neural induction. Dev Biol. 2007; 308:247–256. [PubMed: 17585896]

Massague J, Seoane J, Wotton D. Smad transcription factors. Genes Dev. 2005; 19:2783–2810. [PubMed: 16322555]

Meyers EN, Lewandoski M, Martin GR. An Fgf8 mutant allelic series generated by Cre- and Flp-mediated recombination. Nat Genet. 1998; 18:136–141. [PubMed: 9462741]

Mohammadi M, Honegger AM, Rotin D, Fischer R, Bellot F, Li W, Dionne CA, Jaye M, Rubinstein M, Schlessinger J. A tyrosine-phosphorylated carboxy-terminal peptide of the fibroblast growth factor receptor (Flg) is a binding site for the SH2 domain of phospholipase C-gamma 1. Mol Cell Biol. 1991; 11:5068–5078. [PubMed: 1656221]

Moreau M, Leclerc C, Gualandris-Parisot L, Duprat AM. Increased internal Ca2+ mediates neural induction in the amphibian embryo. Proc Natl Acad Sci U S A. 1994; 91:12639–12643. [PubMed: 7809092]

Neilson JR, Winslow MM, Hur EM, Crabtree GR. Calcineurin B1 is essential for positive but not negative selection during thymocyte development. Immunity. 2004; 20:255–266. [PubMed: 15030770]

Nostro MC, Cheng X, Keller GM, Gadue P. Wnt, activin, and BMP signaling regulate distinct stages in the developmental pathway from embryonic stem cells to blood. Cell Stem Cell. 2008; 2:60–71. [PubMed: 18371422]

O'Keefe SJ, Tamura J, Kincaid RL, Tocci MJ, O'Neill EA. FK506 and CsA-sensitive activation of the interleukin-2 promoter by calcineurin. Nature. 1992; 357:692–695. [PubMed: 1377361]

Pera EM, Ikeda A, Eivers E, De Robertis EM. Integration of IGF, FGF, and anti-BMP signals via Smad1 phosphorylation in neural induction. Genes Dev. 2003; 17:3023–3028. [PubMed: 14701872]

Poteser M, Schleifer H, Lichtenegger M, Schernthaner M, Stockner T, Kappe CO, Glasnov TN, Romanin C, Groschner K. PKC-dependent coupling of calcium permeation through transient receptor potential canonical 3 (TRPC3) to calcineurin signaling in HL-1 myocytes. Proc Natl Acad Sci U S A. 2011; 108:10556–10561. [PubMed: 21653882]

Quadrato G, Benevento M, Alber S, Jacob C, Floriddia EM, Nguyen T, Elnaggar MY, Pedroarena CM, Molkentin JD, Di Giovanni S. Nuclear factor of activated T cells (NFATc4) is required for BDNF-dependent survival of adult-born neurons and spatial memory formation in the hippocampus. Proc Natl Acad Sci U S A. 2012; 109:E1499–1508. [PubMed: 22586092]

Ramel MC, Hill CS. Spatial regulation of BMP activity. FEBS Lett. 2012; 586:1929–1941. [PubMed: 22710177]

Saneyoshi T, Kume S, Amasaki Y, Mikoshiba K. The Wnt/calcium pathway activates NF-AT and promotes ventral cell fate in Xenopus embryos. Nature. 2002; 417:295–299. [PubMed: 12015605]

Sapkota G, Alarcon C, Spagnoli FM, Brivanlou AH, Massague J. Balancing BMP signaling through integrated inputs into the Smad1 linker. Mol Cell. 2007; 25:441–454. [PubMed: 17289590]

Sasai Y, Lu B, Steinbeisser H, De Robertis EM. Regulation of neural induction by the Chd and Bmp-4 antagonistic patterning signals in Xenopus. Nature. 1995; 376:333–336. [PubMed: 7630399]

Schlange T, Andree B, Arnold HH, Brand T. BMP2 is required for early heart development during a distinct time period. Mech Dev. 2000; 91:259–270. [PubMed: 10704850]

Schultheiss TM, Burch JB, Lassar AB. A role for bone morphogenetic proteins in the induction of cardiac myogenesis. Genes Dev. 1997; 11:451–462. [PubMed: 9042859]

Sheng G, dos Reis M, Stern CD. Churchill, a zinc finger transcriptional activator, regulates the transition between gastrulation and neurulation. Cell. 2003; 115:603–613. [PubMed: 14651851]

Spencer DM, Wandless TJ, Schreiber SL, Crabtree GR. Controlling signal transduction with synthetic ligands [see comments]. Science. 1993; 262:1019–1024. [PubMed: 7694365]

Stern CD. Neural induction: old problem, new findings, yet more questions. Development. 2005; 132:2007–2021. [PubMed: 15829523]

Suzuki A, Ueno N, Hemmati-Brivanlou A. Xenopus msx1 mediates epidermal induction and neural inhibition by BMP4. Development. 1997; 124:3037–3044. [PubMed: 9272945]

Tam PP, Loebel DA. Gene function in mouse embryogenesis: get set for gastrulation. Nat Rev Genet. 2007; 8:368–381. [PubMed: 17387317]

Webb SE, Moreau M, Leclerc C, Miller AL. Calcium transients and neural induction in vertebrates. Cell Calcium. 2005; 37:375–385. [PubMed: 15820384]

Wilson SI, Graziano E, Harland R, Jessell TM, Edlund T. An early requirement for FGF signalling in the acquisition of neural cell fate in the chick embryo. Curr Biol. 2000; 10:421–429. [PubMed: 10801412]

Winnier G, Blessing M, Labosky PA, Hogan BL. Bone morphogenetic protein-4 is required for mesoderm formation and patterning in the mouse. Genes Dev. 1995; 9:2105–2116. [PubMed: 7657163]

Wu H, Peisley A, Graef IA, Crabtree GR. NFAT signaling and the invention of vertebrates. Trends Cell Biol. 2007; 17:251–260. [PubMed: 17493814]

Yamaguchi Y, Shinagawa A. Marked Alteration at Midblastula Transition in the Effect of Lithium on Formation of the Larval Body Pattern of Xenopus laevis. Dev Growth Differ. 1989; 31:531–541.

Ying QL, Stavridis M, Griffiths D, Li M, Smith A. Conversion of embryonic stem cells into neuroectodermal precursors in adherent monoculture. Nat Biotechnol. 2003; 21:183–186. [PubMed: 12524553]

Yu PB, Hong CC, Sachidanandan C, Babitt JL, Deng DY, Hoyng SA, Lin HY, Bloch KD, Peterson RT. Dorsomorphin inhibits BMP signals required for embryogenesis and iron metabolism. Nat Chem Biol. 2008; 4:33–41. [PubMed: 18026094]

Zeini M, Hang CT, Lehrer-Graiwer J, Dao T, Zhou B, Chang CP. Spatial and temporal regulation of coronary vessel formation by calcineurin-NFAT signaling. Development. 2009; 136:3335–3345. [PubMed: 19710169]

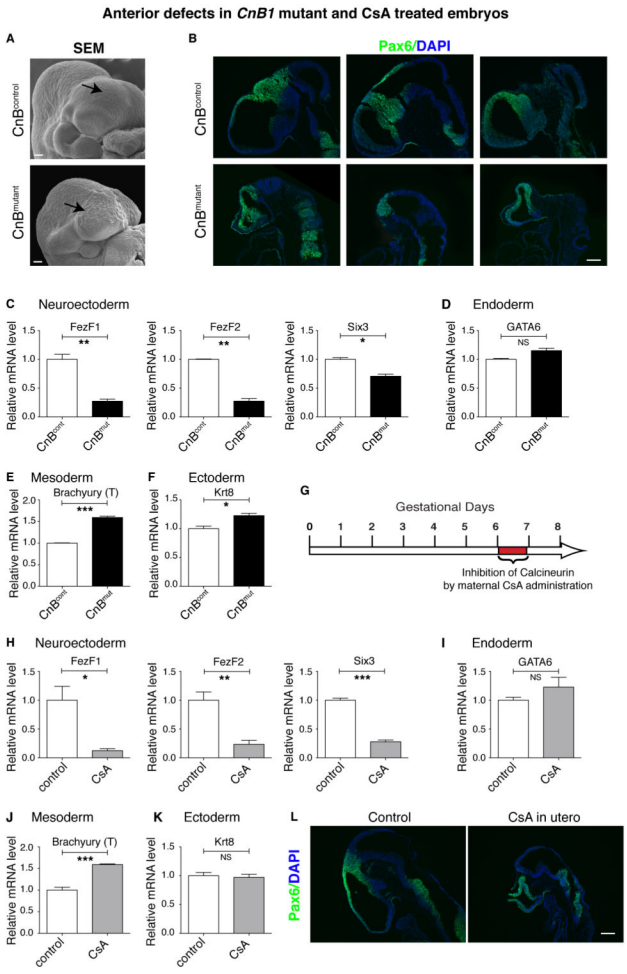

Figure 1. Anterior defects in *CnB1* mutant and CsA treated embryos

(A) Scanning electron micrographs of e9.5 embryos; forebrain (arrow). (B) Pax6 immunostaining of e9.0 sagittal sections. (C-F) qRT-PCR analysis of germ layer markers in e7.5 *CnB1* control and mutant embryos. (C) *Fezf1* (p= 0.0028); *Fezf2* (p=0.0011); *Six3* (p=0.0103). (D) *Gata6* (p=0.0768). (E) *Brachyury* (*T*) (p < 0.0001) (F) *Krt8* (p=0.0295). (G) Cartoon of *in utero* CsA treatment. The red region indicates the critical period during which CaN activity is required in the developing embryo. (H-K) qRT-PCR analysis of germ layer markers in e7.5 control and CsA treated embryos. (H) *Fezf1* (p= 0.0230); *Fezf2* (p=0.0086); *Six3* (p=0.0001). (I) *Gata6* (p=0.2673). (J) *Brachyury* (T) (p = 0.0010) (K) *Krt8* (p=0.7345), (L) *Pax6* immunostaining of e9.0 control and CsA treated embryos. Data are shown as means ± SEM. Scale bars in B&L: 100 μm. See also Figure S1.

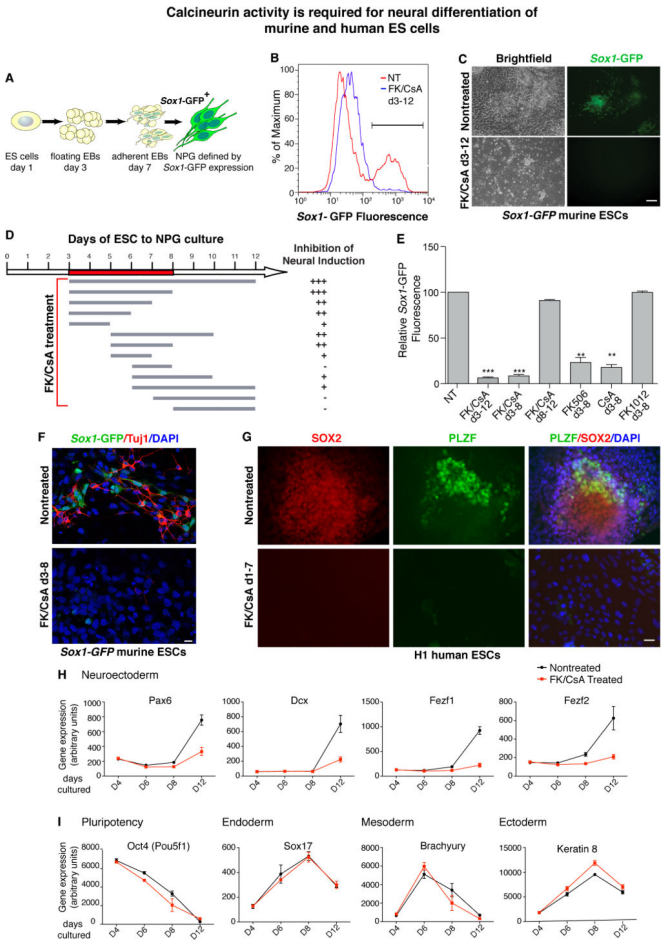

Figure 2. Calcineurin(CaN) activity is required for neural differentiation of murine and human ES cells

(A) Schematic representation of *in vitro* ESC to neural differentiation using *Sox1*-GFP reporter murine ESCs. (B) Quantification of *Sox1*-driven GFP (=*Sox1*-GFP) expression on d12 by FACS analysis. % of GFP positive cells: NT (NT), 27.5%; d3-12 FK506 and CsA-treated, (FK/CsA), 3.84%. (C) *Sox1*-GFP expression of NT and FK/CsA treated (d3-12) cells on d12. (D) Critical time window during which CaN activity is necessary for neural induction. Cells were treated with FK/CsA during the indicated time windows (gray bars) of *in vitro* murine ESC differentiation. On d12, GFP expression of each group was measured by FACS analysis and/or Western blot to quantify neural induction. (E) Quantification of *Sox1*-GFP expression on d12 by FACS analysis (means ± SEM) Cells were treated with indicated molecules during d3-12 or d3-8. FACS data were normalized to the NT control group. p-value compared to NT: FK/CsA d3-12 (n=5), p <0.0001; FK/CsA d3-8 (n=5), p <0.0001; FK506 d3-8 (n=3), p=0.0097; CsA d3-8 (n=3), p= 0.0028. (F) Confocal immunofluorescence images of NT and FK/CsA-treated (d3-8) cells on d15 using antibodies against GFP and pan-neuronal marker β-III-tubulin. Scale bar: 10μm. (G) Immunofluorescence images of NT and FK/CsA-treated H1-cells on d11 of hESC differentiation using antibodies against SOX2 and PLZF. Scale bar: 50μm. (H and I) Microarray gene expression profiles of indicated genes on d4, d6, d8, and d12 cells of *in vitro* murine ESC differentiation. CaN was inhibited with FK/CsA from d3-8. (H) Neuroectoderm markers. (I) Pluripotency, endoderm, mesoderm, and ectoderm markers. Samples were collected from three independent experiments of *in vitro* differentiation. Data are shown as means ± SEM. See also Figure S2.

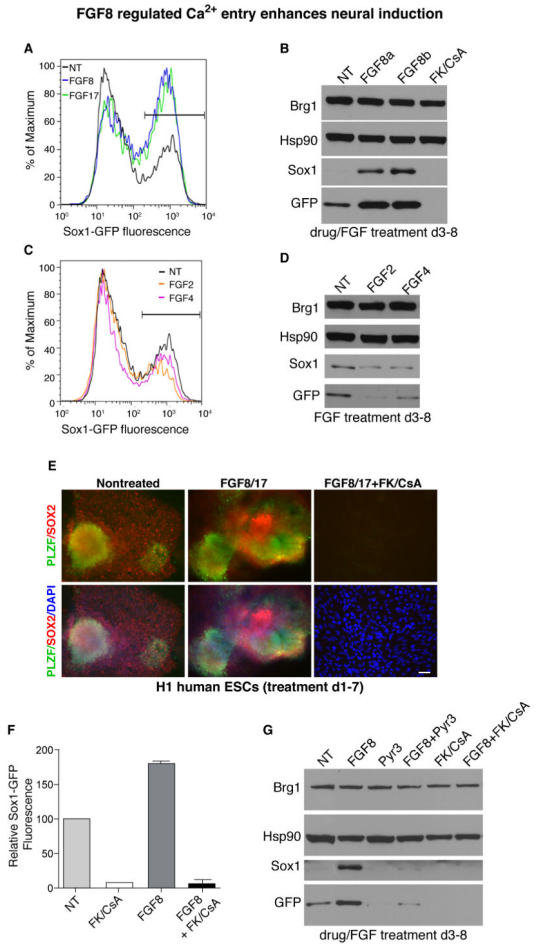

Figure 3. FGF8-regulated Ca^{2+} entry enhances neural induction

(A) Quantification of *Sox1*-GFP expression by FACS. % of GFP positive cells: NT: 32.3%; FGF8: 50.5%; FGF17: 49.5%. (B) Immunoblot analysis of *Sox1*-GFP and Sox1 after treatment with FGF8a, FGF8b or FK/CsA. Brg1 and Hsp90 are loading controls. (C) Quantification of *Sox1*-GFP expression by FACS. % of Sox-1 GFP positive cells: NT: 32.3%; FGF2: 21.9%; FGF4: 30%. (D) Immunoblot analysis of *Sox1*-GFP and Sox1 after treatment with FGF2 and FGF4. (E) SOX2 and PLZF immunostaining of hESC treated with the indicated molecules and harvested on d11 of differentiation. Scale bar: 50μm. (F) Quantification of *Sox1*-GFP expression by FACS analysis (means ± SEM) FACS data were normalized to the NT control group. (G) Immunoblot analysis of GFP and Sox1 expressions after treatment with the indicated molecules. (A-D, F-G) Cells were treated with the indicated growth factors or small molecules during d3-8 of *in vitro* murine ESC differentiation and harvested on d12 for analysis. See also Figure S3.

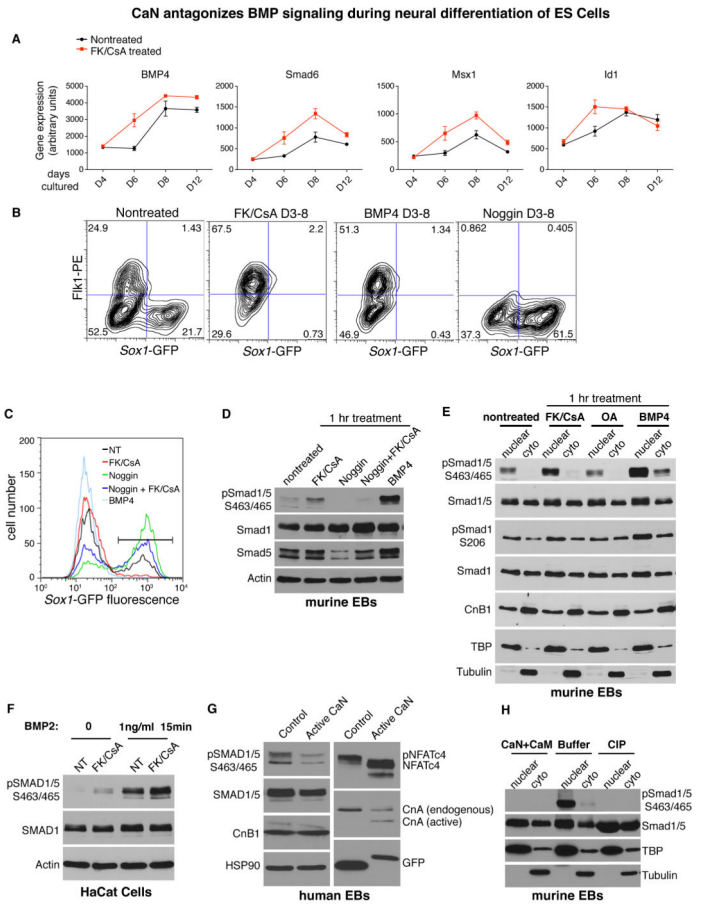

Figure 4. CaN antagonizes BMP signaling during neural differentiation of ESCs

(A-C) Murine ESCs were treated with the indicated molecules from d3 to d8 of *in vitro* differentiation. (A) Microarray gene expression profiles of BMP-regulated genes on d4, d6, d8 and d12. Graphs are shown as means ± SEM. (B) Quantification of *Sox1*-GFP and Flk1 positive cells on d12 by FACS analysis. (C) Quantification of *Sox1*-GFP positive cells on d12 by FACS analysis. % of GFP-positive cells: NT, 27.5%; FK/CsA, 4.68%; Noggin, 74%; Noggin+FK/CsA, 54.2%; BMP4, 0.951%. (D) Immunoblot analysis shows the level of pSmad1/5$^{C\text{-term}}$, Smad1 and Smad5 in d6 EBs treated with the indicated molecules for 1hr. (E) Immunoblot analysis of nuclear and cytoplasmic fractions (d5 EBs) for pSmad1/5$^{C\text{-term}}$, pSmad1^{linker}, Smad1/5, CnB1, TATA-binding protein (TBP) (nuclear loading control) and β-tubulin (cytoplasmic loading control). Cells were treated with the indicated molecules for 1hr. OA: okadaic acid. (F) Immunoblot analysis of HaCaT whole cell extracts for pSmad1/5 $^{C\text{-term}}$, Smad1 and actin. BMP2 and FK/CsA treatment: 15 minutes. (G) The effect of constitutively active CaN on pSmad1/5 $^{C\text{-term}}$ in d2 hEBs differentiated from hESCs expressing control and constitutively active CaN, respectively. Immunoblot analysis shows the level of pSMAD1/5$^{C\text{-term}}$, SMAD1/5, CnB1, NFATc4, CnA, GFP (expression control), and HSP90 (loading control). (H) *in vitro* phosphatase assay using nuclear and cytoplasmic extracts from BMP4-stimulated d8 EBs. Immunoblot analysis detects the levels of pSmad1/5$^{C\text{-term}}$, Smad1/5, TBP, and tubulin after the assay. CIP: Calf intestinal alkaline phosphatase, CaM: CaM. See Experimental Procedures for details. See also Table S1 and Figure S4.

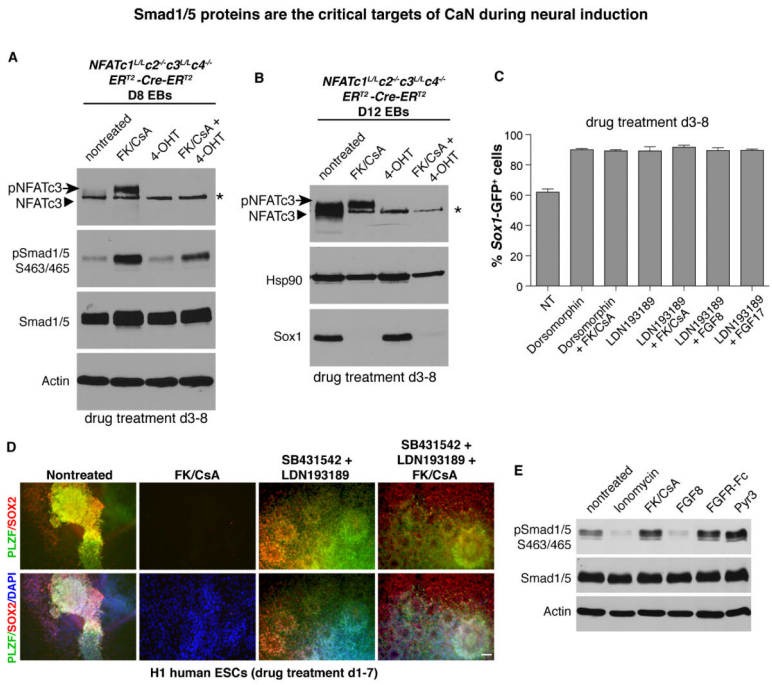

Figure 5. Smad1/5 proteins are the critical targets of CaN during neural induction

(A-B) *in vitro* differentiation of a murine ESC line harboring $ER^{T2}CreER^{T2}$; $NFATc1^{L/L}$ $c2^{-/-}$ $c3^{L/L}c4^{-/-}$ in which the floxed alleles of *NFATc1* and *NFATc3* were removed by 4-OHT-regulated nuclear import of $ER^{T2}CreER^{T2}$. 4-OHT was added at the ESC stage and FK/CsA from d3-8. (A) Immunoblot analysis of d8 EBs using antibodies against NFATc3, pSmad1/5$^{C\text{-term}}$, Smad1/5, and actin (loading control). pNFATc3: phosphorylated (arrow), NFATc3: de-phosphorylated (arrowhead), * indicates a non-specific band. (B) Immunoblot analysis of d12 EBs using antibodies against NFATc3, Sox1, and Hsp90 (loading control). (C) FACS analysis of *Sox1*-GFP expression was used to quantify the percentage of neural induction following inhibition of BMP signaling in the presence or absence of CaN activity or FGF signaling. Cells were treated with indicated molecules during d3-8. FACS data were normalized to the NT control group. (D) Inhibition of CaN has no effect on SOX2 and PLZF expression of hESCs in the presence of dual SMAD inhibition with a combination of SB431542, an ALK inhibitor, and LDN193189, a BMP inhibitor. Scale bar: 50μm. (E) Immunoblot analysis for pSmad1/5$^{C\text{-term}}$, Smad1/5, and actin (loading control) in d4 murine EBs treated with the indicated molecules. Ionomycin, FK/CsA, and FGF8: 1hr, FGFR-Fc and Pyr3: 3hrs. See also Figure S5 and S6.

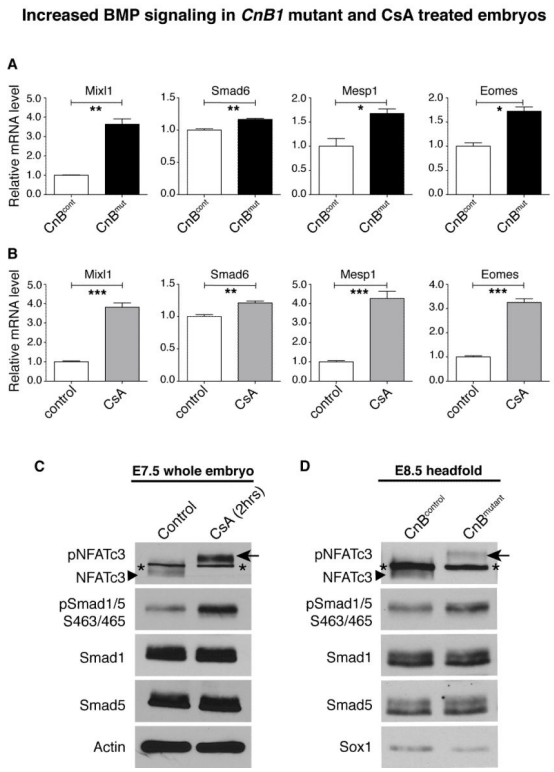

Figure 6. Increased BMP signaling in *CnB1* mutant and CsA treated embryos

A-B) qRT-PCR analysis of BMP-regulated genes at E7.5 (A) *CnB1* control and mutant embryos. *Mixl1* (p=0.0053); *Smad6* (p=0.0030); *Mesp1* (p=0.0214); *Eomes* (p= 0.0108). (B) Control and CsA-treated embryos; pregnant females were injected with CsA on E6.25&6.75.. *Mixl1* (p=0.0002); *Smad6* (p= 0.0073); *Mesp1* (p=0.0006); *Eomes* (p=0.0002). Data are shown as mean ± SEM. (C-D) Immunoblot of NFATc3, pSmad1/5$^{C\text{-term}}$, Smad1, Smad5 and actin in (C) E7.5 control and CsA-treated embryos; (D) e8.0 *CnB1* control and mutant headfolds. pNFATc3: phosphorylated (arrow), NFATc3: dephosphorylated (arrowhead), * indicates a non-specific band.

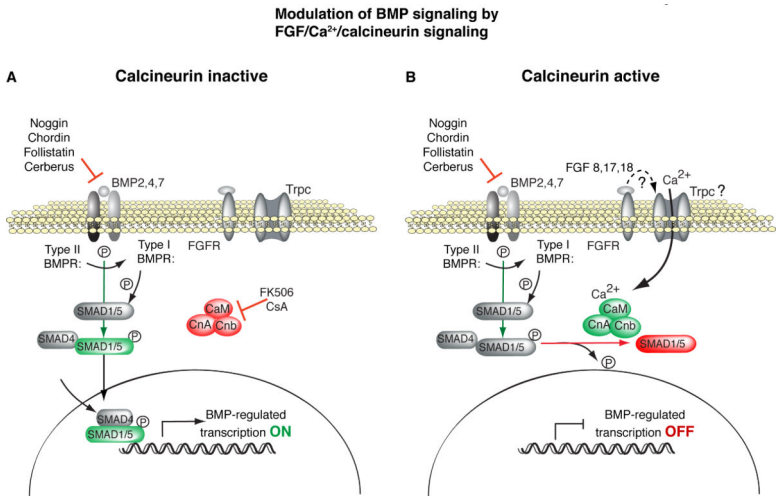

Figure 7. Modulation of BMP signaling by FGF/Ca^{2+}/CaN signaling

Model depicting the proposed mechanism for inhibition of BMP signaling by CaN. FGF signaling triggers an increase of intracellular Ca^{2+}, which activates the CaN phosphatase complex consisting of CnA, CnB, and CaM. Activated CaN specifically dephosphorylates $pSmad1/5^{C\text{-}term}$, thereby opposing BMP signaling. A lack of CaN activity results in an increase of nuclear $pSmad1/5^{C\text{-}term}$ and an enhanced or ectopic activation of BMP-regulated transcription. BMPR, BMP receptor; CnA, calcineurin subunit A; CnB, calcineurin subunit B; FGFR, FGF receptor; TRPC, canonical transient receptor potential.